Temperature-dependent luminescence spectroscopic investigations of U(VI) complexation with the halides F- and Cl-

Demnitz, M.; Hilpmann, S.; Lösch, H.; Bok, F.; Steudtner, R.; Patzschke, M.; Stumpf, T.; Huittinen, N. M.;

Originally published:

May 2020

Dalton Transactions 49(2020), 7109-7122

DOI: https://doi.org/10.1039/D0DT00646G

Perma-Link to Publication Repository of HZDR:

https://www.hzdr.de/publications/Publ-30741

Temperature-dependent luminescence spectroscopic investigations of U(VI) complexation with the halides F^- and Cl^-

M. Demnitz[1], S. Hilpmann[1], H. Lösch[1], F. Bok[1], R. Steudtner[1], M. Patzschke[1], T. Stumpf[1], N. Huittinen[1]*

[1)]Helmholtz-Zentrum Dresden-Rossendorf e.V., Institute of Resource Ecology, Bautzner Landstraße 400, 01328 Dresden, Germany

*Corresponding author :

Nina Huittinen

email : n.huittinen@hzdr.de

phone : +49 351 260 2148

fax : +49 351 260 3553

keywords: uranyl, luminescence, complexation, halides, quenching

Abstract

In the present study we have investigated the complexation of uranyl(VI) with chloride and fluoride using luminescence spectroscopy (TRLFS, time-resolved laser-induced fluorescence spectroscopy). At 25 °C, in the presence of 0 − 0.175 M fluoride, the first single-component emission spectra for all four U(VI)-fluoride complexes, i.e. UO_2F^+, UO_2F_2, $UO_2F_3^-$, and $UO_2F_4^{2-}$ could be extracted. Based on the aqueous speciation derived from the TRLFS data, log*K** values at I = 1 M were calculated for all these complexes and extrapolated to infinite dilution using the SIT approach. In the case of chloride, however, quenching of the U(VI)-luminescence hampered the experiments. Thus, U(VI)-complexation was studied with TRLFS at liquid nitrogen temperatures. Samples were prepared at 25 °C with chloride concentrations ranging from 0 to 1.0 M followed by instantaneous freezing and subsequent luminescence spectroscopic measurements at −120 °C. This allowed for the determination of the first luminescence spectra for the UO_2Cl^+ complex with the TRLFS method. The chloride quench reaction was further studied in the temperature range 1 – 45 °C using Stern-Volmer analysis. By applying the Arrhenius and the Eyring equations we obtained the first thermodynamic parameters for the dynamic quench process, i.e. the activation energy (E_a = 55.0 ± 12.9 kJ/mol), enthalpy ($\Delta H^{\ddagger}$ = 52.5 ± 13.0 kJ/mol), and entropy ($\Delta S^{\ddagger}$ = 103.9 ± 42.8 J/mol·K).

1 Introduction

Uranyl(VI) complexation in aqueous solution with inorganic and organic ligands have an influence on the retention behavior and therefore, on the mobility and (bio)availability of U(VI) in the environment. The halides are an important group of elements to be considered in such U(VI)-complexation reactions. Chloride is the most abundant inorganic ligand in our water reservoirs and in natural salt deposits[1]. It is also one of the most important constituents in the pore waters of crystalline rock[2] and clay[3] in subsurface formations. In addition, the strong halide ligand fluoride, is present in several minerals such as fluoroapatite and fluorite, which are frequently encountered in crystalline rock formations such as granite.[4, 5] Complexed uranyl(VI) with fluoride is further a trace indicator for the uranium enrichment process, as the produced UF_6 in contact with moist air will form uranyl(VI) fluoride under oxic conditions.[6, 7]

Several studies dedicated to uranyl(VI) complexation reactions with the above-mentioned halide ligands and the extraction of complexation constants for the formed U(VI)-halide complexes, have been conducted at ambient conditions.[8-14] In addition, few studies report on complexation investigation at elevated temperatures[15, 16], which are of relevance in deep subsurface environments[17] related to e.g. geothermal energy production or in the vicinity of heat-generating spent nuclear fuel repositories.[18] Published complexation constants at various temperatures were compiled in Table S1 and Table S2 in the supporting information (SI) for U(VI)-fluoride and U(VI)-chloride complexes, respectively. These constants were derived with various indirect methods using ion selective electrodes[9, 19, 20] or cation exchange[10], and direct spectroscopic methods including spectrophotometry[11-13, 16] and NMR.[21] The use of time-resolved laser-induced luminescence spectroscopy (TRLFS) has only been used in a few studies[15] for the derivation of U(VI)-halide complexation constants despite its low detection limits and the excellent luminescent properties of U(VI) allowing for the direct *in situ* monitoring of complexation reactions in aqueous environments. For the fluoride ligand, luminescence studies are limited to the early U(VI)-fluoride complexes, UO_2F^+ and UO_2F_2, prevailing at low total fluoride concentrations. In the presence of chloride, no luminescence spectra have been published for U(VI)-chloride complexes and consequently TRLFS has not been used for the derivation of any U(VI)-chloride complexation constants. The lack of luminescence data for chloride-containing solutions can be traced back to the severe quenching of the luminescence emission in the presence of this halide. The quenching has been proposed to occur through electron transfer from chloride to uranyl(VI), resulting in the formation of a non-luminescent U(V)-like transition state.[22-25] The quenching has been shown to occur already at very low total chloride concentrations, where no UO_2Cl^+ complexes are present in solution,

implying that dynamic quenching plays a crucial role in the quench-reaction. At higher total chloride concentrations additional static quenching by the formed UO_2Cl^+ complex can be assumed to occur. Temperatures below the freezing point have been shown to decrease dynamic quenching effects. Samples can easily be cooled down to temperatures of −196 °C and −269 °C by use of liquid nitrogen and liquid helium, respectively. When rapid cooling is undertaken, *i.e.* when a sample prepared at room temperature is directly immersed in liquid nitrogen, the chemistry prevailing at ambient conditions should be preserved due to the very low reaction rates at these low temperatures.[26, 27] This allows for luminescence spectroscopic investigations of systems containing quenching ligands, such as chloride.

In the present study we have investigated the complexation of uranyl(VI) with chloride and fluoride using TRLFS. The fluoride concentration range has been chosen so, that also higher U(VI)-fluoride complexes ($UO_2F_3^-$ and $UO_2F_4^{2-}$) are present in solution in addition to the already reported UO_2F^+ and UO_2F_2 ones, allowing the extraction of spectroscopically derived complexation constants for all above-mentioned complexes at 25 °C. As the chloride quenching phenomenon can be overcome by cooling down the samples to liquid nitrogen temperatures, U(VI)-chloride samples initially prepared at 25 °C have been frozen and measured at −120 °C using a liquid nitrogen jet stream for the derivation of the first UO_2Cl^+ luminescence spectra with the TRLFS method. The spectra of the UO_2F^+ and UO_2Cl^+ were compared to draw analogies. Finally, due to the role of temperature in the quench process chloride and fluoride complexation in the temperature-range from 1 °C to 45 °C have been studied. From the observed chloride-induced quench reaction, constants for the dynamic and static quench processes using the Stern-Volmer equations[28] could be derived in addition to thermodynamic data, *i.e.* the activation energy, enthalpy, and entropy.

2 Materials and methods

2.1 Sample preparation

Uranyl(VI) stock solutions were prepared by converting $UO_2(NO_3)_2 \cdot 6\ H_2O$ (Merck KGaA) to uranyl peroxide using H_2O_2 solution, which was heated in contact with air at 350 °C to obtain $UO_3 \cdot 2\ H_2O$. The uranium oxide was dissolved in concentrated $HClO_4$ and thereafter diluted with deionized water to a final concentration of 0.1 M UO_2^{2+} in 0.5 M $HClO_4$. All other high purity reagent grade materials were used without any further treatment. NaCl (> 99.5 %; Merck KGaA) and HF (48 %; Carl Roth GmbH + Co. KG) were used in the preparation of solutions containing chloride and fluoride, respectively. $NaClO_4 \cdot H_2O$ (> 99 %; Merck KGaA) served as a background electrolyte. Milli-Q water was used in the dilution of all samples.

For the correct adjustment of the sample pH to the desired total proton concentration [H] in the rather high background electrolyte concentrations used in the present work, a correction of the experimental pH_{exp} by an empirical coefficient A_c according to equation (1) is required.

$$-\log[H^+] = pH_{exp} + A_c \quad (1)$$

A_c was determined by an empirical equation published by Jordan et al (2018).[29] To avoid $KClO_4$ precipitation and unwanted chloride contamination a double junction electrode from Metrohm was prepared, using 3 M KCl in the inner chamber and 3 M $NaClO_4$ in the outer chamber. pH electrode calibration was performed using standard WTW buffer solutions.

To study the temperature-dependent complexation between uranyl(VI) and fluoride, solutions containing a constant U(VI) concentration of 0.1 mM and fluoride concentrations between 0 and 0.175 M were prepared at a constant pH of 2 ([H] = 0.01) and an ionic strength of 1 M was adjusted with $NaClO_4$. The samples were equilibrated at the desired temperatures (1 to 45 °C) using thermoelements from Quantum Northwest.

For luminescence spectroscopic studies of U(VI)-chloride complexation at liquid nitrogen temperatures (−120 °C, 153 K) uranyl(VI) chloride samples with [U] = 0.04 mM and [Cl] = 0 – 1.0 M were prepared at a constant pH of 1.4 ([H] = 0.040). The overall ionic strength was kept constant at 1.1 M using $NaClO_4$. At a temperature of 1 °C, the uranyl(VI) chloride speciation was investigated in solutions containing [U] = 5 mM with [Cl] ranging from 0 to 0.5 M, I = 0.5 M and −log[H] = 0.5 and 2.5. The quenching of U(VI) luminescence in the presence of chloride for the derivation of thermodynamic data of the quench process was investigated in solutions containing [U] = 0.1 mM with [Cl] = 0 – 0.01 M at −log[H] = 1 and I = 0.11 M at temperatures ranging from 1 to 45 °C. Similarly to the fluoride samples,

thermocouples from Quantum Northwest were used to equilibrate the samples at the desired temperatures.

2.2 Time-resolved laser-induced luminescence spectroscopy

The speciation of uranyl(VI) can be monitored via the detection of the uranyl(VI) luminescence. The change of the coordination environment of uranyl(VI) will result in the spectral shift and change of intensity of its characteristic luminescence emission signals. The luminescence spectroscopic investigations in the temperature-range 1 – 45 °C were conducted by transferring 3 ml of the sample volume into a quartz glass cuvette. For the uranyl(VI) chloride series at −120 °C a 1 ml aliquot was frozen instantly in plastic cuvettes using liquid nitrogen. The sample was kept at −120 °C during the measurements using a jet stream of liquid nitrogen. Laser spectroscopic measurements were performed using nanosecond Nd:YAG lasers (Continuum Minilite I and Continuum Minilite II; Continuum Electro-Optics Inc.) as an excitation source in the 1 – 45 °C experiments, while Continuum Inlite; Continuum Electro-Optics Inc. was used in the liquid nitrogen experiments. Luminescence spectra were recorded at 425 – 625 nm at a delay of 40 to 135 ns after the excitation impulse, depending on the experiment, with a constant excitation wavelength of 266 nm. For time-resolved measurements luminescence spectra were recorded step-wise every 5 to 50 ns after the excitation pulse depending on the measured sample.

2.3 Determination of complexation constants

Conditional constants log$K$* can be determined from the spectroscopically derived U(VI)-fluoride and U(VI)-chloride species distributions using slope analysis. Hereby the logarithmic concentration of the ligand [L] is plotted against the logarithmic ratio of the reaction product [RL] and the reactant molecule [R] according to formula (3) derived from formula (2). The slope a corresponds to the number of reacting ligands, while the intercept with the y-axis yields the logarithmic conditional complexation constant log$K$*.

$$[\mathrm{R}] + a[\mathrm{L}] \rightleftharpoons [\mathrm{RL_a}] \tag{2}$$

$$\log\left(\frac{[\mathrm{RL}]}{[\mathrm{R}]}\right) = a \cdot \log([\mathrm{L}]) + \log(K^*) \tag{3}$$

The ligand concentration [L], i.e. the concentration of free F^- and Cl^- in solution was calculated using the PHREEQC program Version 3.4.0.[30] The calculations were based on the Thermochimie V9.0 SIT database from ANDRA.[31, 32] Further needed SIT parameters were taken from literature (see Table S3 and S4).[33, 34] For the calculations a temperature of 25 °C and an ionic strength of 1 M (F^- samples) or 1.1 M (Cl^- samples) $NaClO_4$ were used. Molar values were converted to the molal scale using density values listed in the Thermochimie V9.0 SIT database. The reaction product [RL] and the remaining uranium concentration in solution [R] were derived from the species distribution obtained from TRLFS data. The spectroscopically derived species distribution for the U(VI)-fluoride and chloride systems were compared with calculated distributions, based on average values of reported complexation constants for the various U(VI)-fluoride/chloride complexes. The distribution was determined using a uranium concentration of 0.1 mM (in F^- media) or 0.04 mM (in Cl^- media).

3 Results

3.1 Uranium(VI) complexation with fluoride at 25 °C

The luminescence emission spectra of U(VI) in the presence of fluoride at 25 °C are presented in Figure 1 a). A constant red shift of the uranyl(VI) signal with increasing fluoride concentration can be seen as a result of progressing complexation in solution.

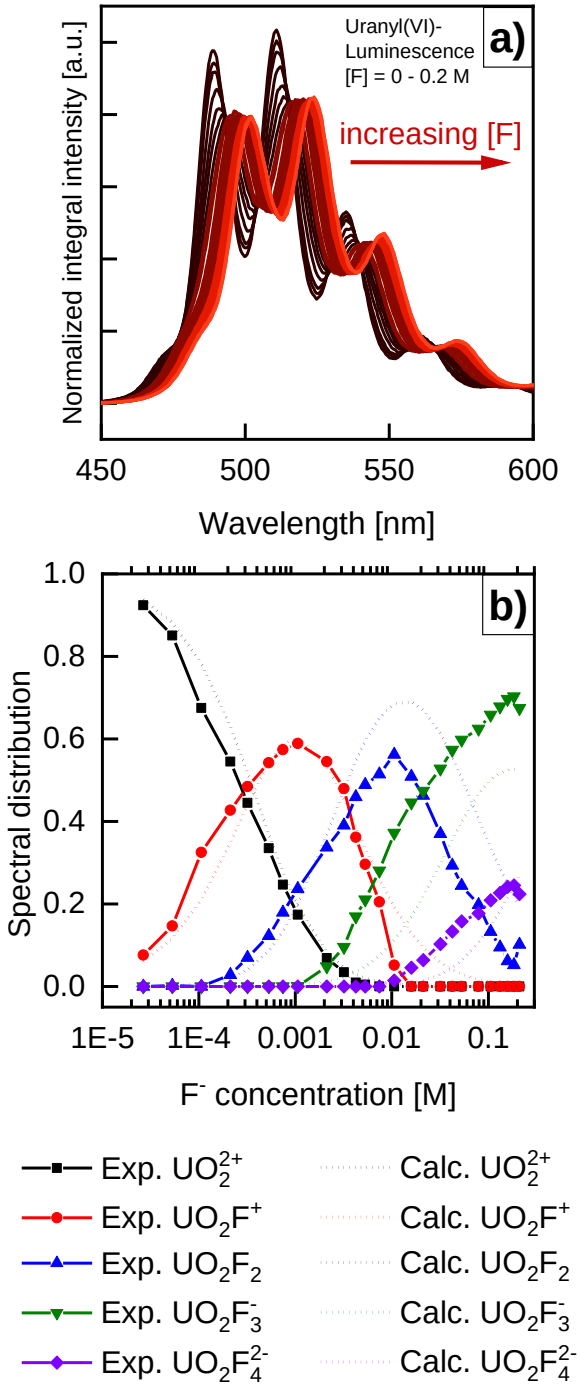

Figure 1: **a)** Luminescence spectra of uranyl(VI) with increasing fluoride concentration [F] = 0 – 0.175 M; −log[H] = 2; I = 1 M; T = 25 °C and **b)** Calculated and spectroscopically derived speciation of uranyl(VI) in the aqueous system in dependence of the fluoride concentration at −log[H] = 2, I = 1 M at 25 °C.

Using spectral deconvolution, the collected composite spectra could be described by four U(VI)-fluoride species (species 1 – species 4) in addition to the free uranyl(VI) aquo ion (UO_2^{2+}), see Figure 2 and Figure S2 in the supplementary information (SI). A comprehensive discussion of the deconvolution process can be found in Huittinen et al.[35] The single component spectra of the complexes were then smoothed using a 5 to 6 point FFT (Fast Fourier Transform) due to a poor signal-to-noise ratio of the extracted components.

Based on the peak positions of the extracted components, the emission spectra of the two first fluoride species compare very well with already existing data for UO_2F^+ and UO_2F_2, see Table 1.[15] Thus, species 1 and species 2 can tentatively be assigned to these two above-mentioned fluoride complexes.

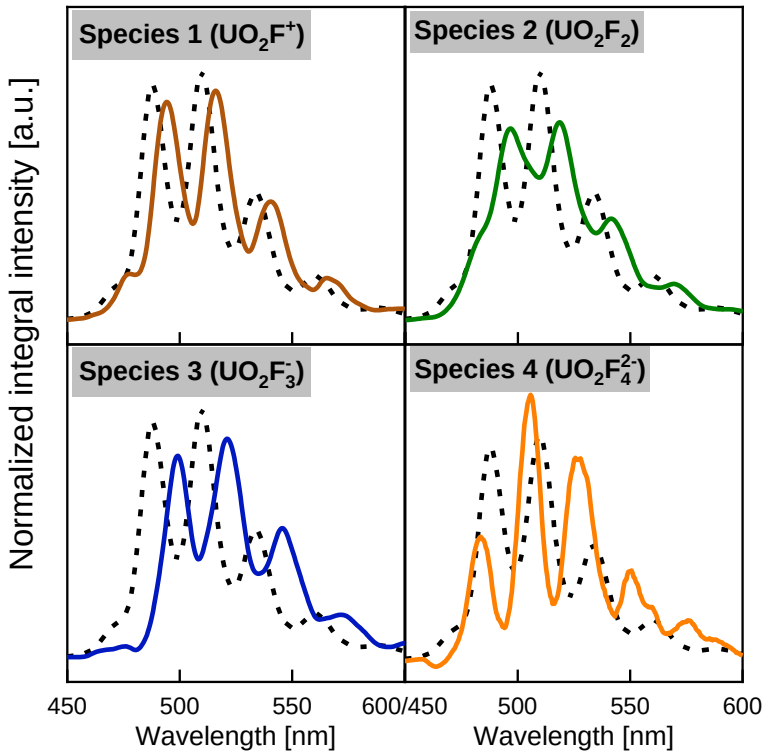

Figure 2: Single component spectra of UO_2^{2+} (black dashed line), species 1, species 2, species 3 and species 4 extracted from fluoride-containing solutions [F] = 0 – 0.175 M; −log[H] = 2; I = 1 M; T = 25 °C.

To gain further insight into the U(VI)-fluoride speciation in solution, a relative species distribution was calculated based on the extracted pure component spectra.

Table 1: Main emission peaks of the single component spectra of the uranyl(VI) fluoride complexes.

Component	Peak I [nm]	Peak II [nm]	Peak III [nm]	Literature
UO_2^{2+}	488.1 ± 0.1	509.9 ± 0.1	533.7 ± 0.1	This work
Species 1 (UO_2F^+)	494.5 ± 0.1	516.3 ± 0.1	540.3 ± 0.1	
Species 2 (UO_2F_2)	496.8 ± 0.1	518.7 ± 0.1	542.3 ± 0.1	
Species 3 ($UO_2F_3^-$)	499.0 ± 0.1	521.0 ± 0.1	545.8 ± 0.1	
Species 4 ($UO_2F_4^{2-}$)	505.3 ± 0.1	527.4 ± 0.1	550.6 ± 0.2	
UO_2^{2+}	488	510	533	Kirishima et al.[15]
UO_2F^+	495	517	541	
UO_2F_2	498	520	544	

For this, relative luminescence intensity (LI) factors for the present species had to be calculated (see Table S6). They take into account the differences in luminescence quantum yields of the various species relative to the non-complexed uranyl(VI) aquo ion. A detailed description of the LI factor calculation can be found in literature.[35]

Using the obtained LI factors and the single component spectra it was possible to calculate the speciation of uranyl(VI) in dependence of the fluoride concentration (−log[H] = 2, I = 1 M) at room temperature applying the least squares fitting method. The obtained results in Figure 1 b) were compared to calculations determined by PHREEQC using existing complexation constants for U(VI)-fluoride complexes. Figure 1 b) shows that the calculated and experimentally derived species distributions in dependence of the fluoride concentrations are in general agreement with each other. Thus, we can primarily assign the four U(VI)-fluoride species to the four progressing $UO_2F_n^{2-n}$ complexes, with *n* being the number of fluoride ligands ranging from 1 to 4. Each new fluoride complexing the uranyl(VI) induces an additional red shift of the luminescence emission. Starting with UO_2F_2 the spectroscopically derived species distribution seems to differ slightly from the calculated species distribution. To verify the proposed stoichiometry of the complexes as well as to determine the conditional complexation constants we performed a slope analysis using the calculated F^- concentrations.

Slope analysis was applied to all species using equation (3). The slope obtained for species 1, assuming the reaction $UO_2^{2+} + F^- \rightleftharpoons UO_2F^+$, is 1.00 ± 0.04 as shown in Figure 3 and it indicates a one step reaction between the uranyl(VI) cation and one fluoride ligand resulting in the formation of the proposed UO_2F^+ complex. The intercept with the y-axis yields the conditional complexation constant log*K** at I = 1 M, which is in very good agreement with published data for this complex, see Table 2. Further slope analyses were performed for the other species, confirming the existence of the proposed $UO_2F_n^{2-n}$ complexes to the different species

respectively. The corresponding slope analyses based on the equations in Table 2 can be found in the SI (Figure S5).

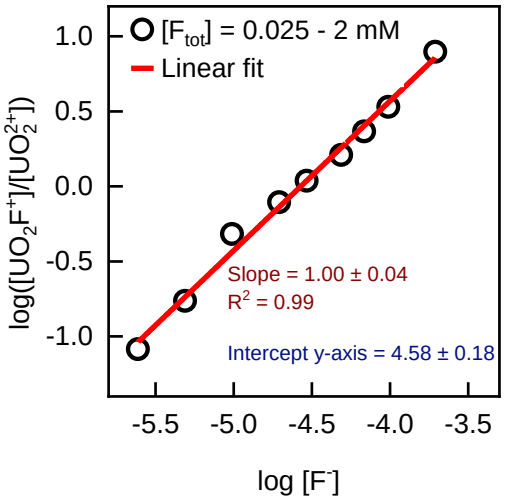

Figure 3: Slope analysis for the UO_2F^+ complex according to equation (3) assuming the reaction $UO_2^{2+} + F^- \rightleftharpoons UO_2F^+$.

The obtained results and a comparison to known literature values are shown in Table 2. The literature values are average values of complexation constants for the respective U(VI)-fluoride complexes recommended by the NEA-TDB (for more details, see the SI). For the experimentally determined slope and log$K$* values, the error range was determined using two times the standard deviation of the data sets. LogK^0 values were determined using SIT equations suggested by NEA using values listed in Table S4.[34]

Table 2: Used reactions for the slope analysis, the obtained slope and a comparison of experimentally determined log$K$* values (this study) with literature values for uranyl(VI) fluoride complexes at I = 1 M and T = 25 °C.

Reaction scheme	Slope	Exp. log$K$* (logK^0)	Lit. log$K$*
$UO_2^{2+} + F^- \rightleftharpoons UO_2F^+$	1.00 ± 0.04	4.58 ± 0.18 (5.19)	4.54 ± 0.03[9, 19, 20, 36]
$UO_2F^+ + F^- \rightleftharpoons UO_2F_2$	1.02 ± 0.20	3.59 ± 0.67 (3.69)	3.40 ± 0.09[9, 19, 20, 36]
$UO_2F_2 + F^- \rightleftharpoons UO_2F_3^-$	1.02 ± 0.07	2.77 ± 0.17 (2.60)	2.39 ± 0.39[8, 9, 19, 20, 36]
$UO_2F_2 + 2\ F^- \rightleftharpoons UO_2F_4^{2-}$	2.05 ± 0.34	4.41 ± 0.65 (4.05)	3.68 ± 0.79[8, 9, 19, 36]
$UO_2F_3^- + F^- \rightleftharpoons UO_2F_4^{2-}$	---	1.64 ± 0.67 (1.45)[1]	

[1]*Calculated from the logK* values of the $UO_2F_2 + 2\ F^- \rightleftharpoons UO_2F_4^{2-}$ and $UO_2F_2 + F^- \rightleftharpoons UO_2F_3^-$ reactions.*

Table 2 shows that the slope corresponds to the number of fluoride ligands taking part in the proposed reaction. The log$K$* values obtained in this work are slightly higher in comparison to literature values. It is not unreasonably to assume the difference might be due to the use of a sensitive spectroscopic method. Tian et al. (2009) determined log$K$* values for the $UO_2F_n^{2-n}$ (n = 1 – 4) complexes at I = 1 M and T = 25 °C using spectrophotometry. Their complexation constants were moderately higher than the values suggested by NEA (1992), see Table S1. Their values (log$K$* (I = 1 M) $UO_2F^+/UO_2F_2/UO_2F_3^-/UO_2F_4^{2-}$ = 4.60 / 8.07 / 10.78 / 11.92) are

very similar to ours (log*K** (I = 1 M) = 4.58 / 8.17 / 10.94 / 12.58), suggesting a slightly enhanced fluoride complexation behavior than previously reported.

Finally, having extracted pure component spectra for all four U(VI)-fluoride complexes (Figure *2*), changes in the total symmetric stretch vibration frequency (ν_s), of the uranyl moiety as a function of the number of fluoride ligands could be calculated. The stretch vibration frequency can be obtained from the spacing between the electronic transition line E, and the higher vibronic level S_1 of the electronic ground state. Therefore, the peak positions of the first and second peak emission peaks of the extracted pure component spectra were recalculated to obtain their respective wavenumbers (see Table S5). The wavenumber and the stretch vibration frequency show a linear decrease with increasing fluoride ligand number in Figure S3 and Figure S4, respectively, which is an indication of a systematic weakening of the U=O bond by the coordination of the strongly donating fluoride ligands in the equatorial plane. The linear fit of the stretch vibration frequency as a function of fluoride complexation resulted in the following expression (4):

$$\nu_S(cm^{-1}) = -11\ cm^{-1} \cdot n(F^-) + 870\ cm^{-1} \quad (4)$$

A similar electron donating effect resulting in a linear relation between ν_s and the number of coordinating ligands was previously reported for U(VI)-hydroxyl species ($\nu_S(cm^{-1}) = -22\ cm^{-1} \cdot n(OH^-) + 870\ cm^{-1}$).[37]

3.2 Complexation of uranyl(VI) with chloride

Chloride complexation with uranyl(VI) was investigated using liquid nitrogen at −120 °C to overcome the quenching of the uranyl(VI) luminescence through chloride. Similar to the complexation with fluoride, chloride induces a continuous red shift of the uranyl(VI) luminescence (see Figure *4* a). The red shift indicates progressing complexation of the uranyl(VI) with chloride as the ligand concentration increases.

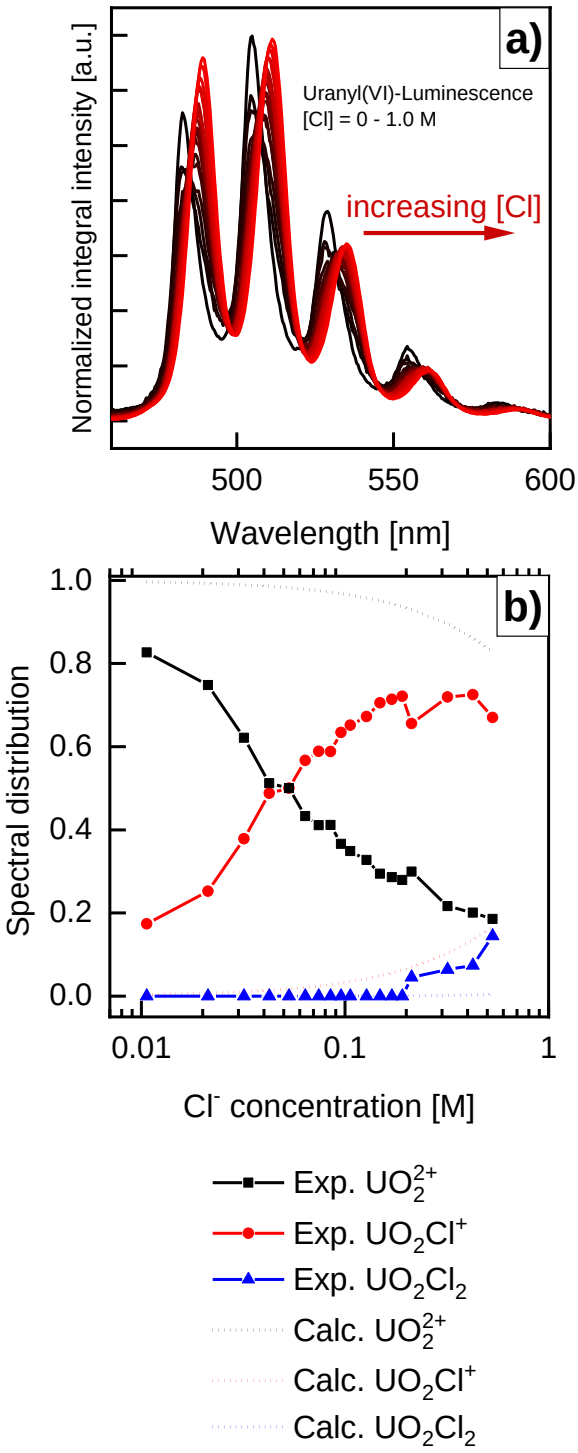

Figure 4: **a)** Luminescence spectra of uranyl(VI) with increasing chloride concentration [Cl] = 0 – 1.0 M; −log[H] = 1.5; I = 1.1 M; T = −120 °C and **b)** calculated and uncorrected spectroscopically derived speciation of uranyl(VI) in the aqueous system in dependence of the chloride concentration at −log[H] = 1.4, I = 1.1 M at 25 °C.

To determine the species in solution peak deconvolution was performed. From the individual spectra three single component spectra could be determined (see Figure S6 in the SI). The first component is the free uranyl(VI) aquo ion, however, at −120 °C it is blue shifted in comparison to the aquo ion at 25 °C (see Table 3). The blue shift is slightly more pronounced for peak I (4.7 nm, 174 cm^{-1}) than peak III (4.1 nm, 166 cm^{-1}). This blue shift has been observed to

increase with decreasing temperature, but the underlying reasons for it are not well understood.[38] The two other pure components extracted from the composite spectra measured in the chloride containing solutions must belong to U(VI)-chloride complexes, i.e. the UO_2Cl^+ complex (species 1) and UO_2Cl_2 (species 2) (see Figure S6). Species 1 is present already at rather low chloride concentrations of 10 mM, while species 2 appears at chloride concentrations exceeding 0.2 M. The resulting, uncorrected species distribution is presented in Figure 4 b), right, together with a calculated species distribution based on published complexation constants from the NEA-TDB.[33] The uncorrected experimental and calculated species distributions differ very strongly from one another. A correction of the species distribution, however, could not be done, as the LI factor determination was unsuccessful. Generally the luminescence intensity increases with increasing chloride concentration (Figure S7), but light scattering from the frozen samples is very incongruent. This results in very different luminescence intensities between the samples which subsequently hampers an accurate determination of the LIs, which is unfortunate as the speciation depends strongly on these LI factors.

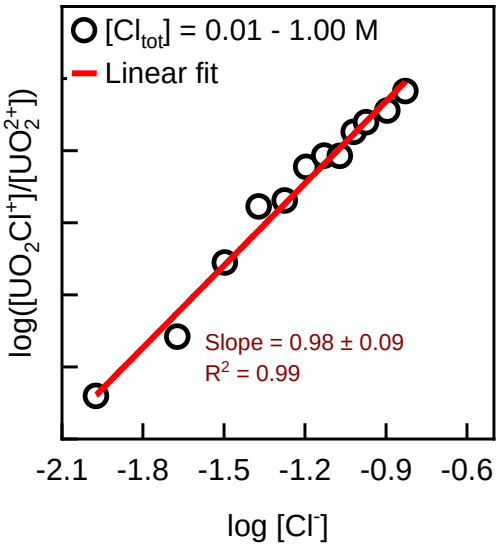

Figure 5: Slope analysis for the UO_2Cl^+ complex according to equation (3) assuming the reaction $UO_2^{2+} + Cl^- \rightleftharpoons UO_2Cl^+$.

Nevertheless, the stoichiometry of the formed complexes can be extracted from the uncorrected species distribution by slope analysis. Due to the low amount of samples (only 5) for which the second species is present, slope analysis was successful only for the first chloride complex. The results of the slope analysis is presented in Figure 5.

Table 3: Main emission peaks of the single component spectra of the uranyl(VI) halide complexes.

Component	Peak I [nm]	Peak II [nm]	Peak III [nm]	Literature
UO_2^{2+} (−120 °C)	484.0 ± 0.1	505.6 ± 0.1	529.0 ± 0.1	This work
Species 1 (UO_2Cl^+) (−120 °C)	488.6 ± 0.1	510.6 ± 0.1	534.5 ± 0.1	
Species 2 (UO_2Cl_2) (−120 °C)	490.1 ± 0.1	512.1 ± 0.1	536.0 ± 0.1	
UO_2^{2+} (25 °C)	488.1 ± 0.1	509.9 ± 0.1	533.7 ± 0.1	
UO_2F^+ (25 °C)	494.5 ± 0.1	516.3 ± 0.1	540.3 ± 0.1	

The slope analysis results in a slope of 0.98 ± 0.09, indicating a one-step reaction between the uranyl(VI) cation and the chloride ligand, which confirms that species 1 is the UO_2Cl^+ complex. This is the first pure component spectrum for a U(VI)-chloride complex obtained with the TRLFS method. Having seen complex formation in a frozen state at −120 °C, it is of interest to investigate complex formation in the aqueous state. While no complex formation of uranyl(VI) ([U] = 0.1 mM) in a solution containing chloride [Cl] = 0 – 0.05 M at room temperature could be observed due to severe quenching, it was possible to measure a uranyl(VI) luminescence at 1 °C in solution. With increasing chloride concentration a red shift of the luminescence signal was obvious (Figure S8) and a peak deconvolution, similar to the procedure for the uranyl(VI) fluoride complexes, was possible. Hereby we obtained the first single component spectrum for the UO_2Cl^+ complex in the aqueous state using TRLFS (see Figure 6). A rather similar redshift of the UO_2Cl^+ complex at 1 °C in comparison to −120 °C as seen for the aquo ion at 25 °C and −120 °C can be observed (see Table 4). Therefore, the UO_2Cl^+ spectrum at −120 °C has been shifted by the amount the aquo ion shifts between −120 °C and 25 °C in Figure 6 to allow direct comparison of the halide spectra measured at different temperatures. For the non-shifted spectrum of UO_2Cl^+ at −120 °C see Figure S6 in the SI.

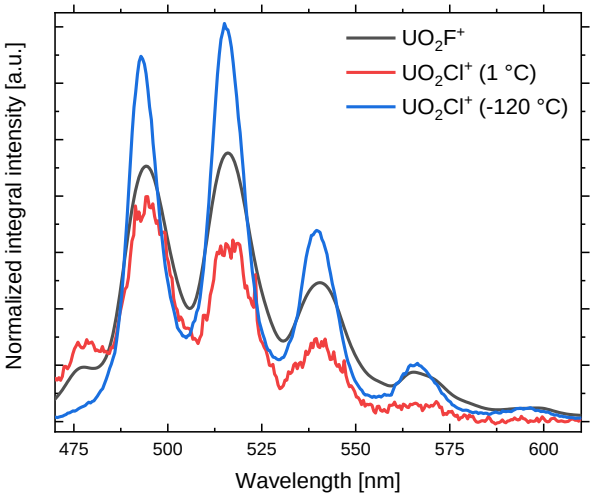

Figure 6: Comparison of the single component spectra of the UO_2F^+ complex at 25 °C, UO_2Cl^+ complex at 1 °C and – 120 °C.

Despite some discrepancies regarding the relative intensities of the emission peaks, it is clear that the UO_2Cl^+ spectra measured at the two different temperatures and the UO_2F^+ spectrum are very similar. The peak positions are almost identical in all cases speaking for the formation of a very similar 1:1 halide complex both in the presence of chloride and fluoride.

Table 4: Main emission peaks of the single component spectra of the uranyl(VI) halide complexes.

Component	Peak I [nm]	Peak II [nm]	Peak III [nm]	Literature
UO_2Cl^+ (1 °C)	495.1 ± 0.1	516.7 ± 0.1	540.4 ± 0.1	This work
UO_2Cl^+ (−120 °C)	489.5 ± 0.1	511.5 ± 0.1	535.3 ± 0.1	
UO_2F^+ (25 °C)	494.5 ± 0.1	516.3 ± 0.1	540.3 ± 0.1	

3.3 Influence of temperature and halides on uranyl(VI) luminescence behavior

At ambient conditions, no quenching of the uranyl(VI) luminescence signal in the presence of fluoride has been observed.[22-24] It has been suggested, however, that the strong oxidizing potential of $UO_2F_4^{2-}$ is accompanied by luminescence quenching effects in the presence of redox-sensitive ligands.[39] Thus, the luminescence behavior of U(VI) in fluoride-containing solutions was studied at selected fluoride concentrations in the temperature range between 1 °C and 45 °C. As shown in Figure 7, at lower fluoride concentrations of [F] = 0.1 mM, increasing the temperature from 1 to 25 °C results in a drop of the luminescence intensity. At this low fluoride concentration, the majority of the luminescence signal stems from the U(VI) aquo ion. The loss of intensity can thus be traced back to a stronger thermal quenching effect of the water molecules coordinating to UO_2^{2+} due to their thermal vibrations.[40] Beyond 25 °C, the relative luminescence intensity in comparison to the aquo ion is greater, even in the presence of this

very low amount of fluoride (0.1 mM). This implies that the thermal quenching by coordinating water molecules has decreased as a result of an enhanced formation of the UO_2F^+ and UO_2F_2 complexes with increasing temperature. The higher intensity of the complexes is due to the replacement of water molecules in the coordination sphere by the fluoride ligand, decreasing the quenching effect by water. The enhanced complexation at this fluoride concentration can also be seen in Figure 7 a), as a systematic red-shift of the luminescence signal with increasing temperature. The red-shift is much more pronounced than observed for the U(VI) aquo ion (see SI, Figure S9). This points toward an endothermic reaction enthalpy of the formed UO_2F^+ and UO_2F_2 complexes, in agreement with literature.[41] Further, no indications of luminescence quenching at any of the investigated temperatures can be established. Increasing the temperature in the same range at higher fluoride concentrations of [F] = 10 mM (Figure 7 b) can be seen to further increase the relative luminescence intensity in comparison to the aquo ion. The increase is a result of the formation of the $UO_2F_3^-$ and $UO_2F_4^{2-}$ complexes and further replacement of coordinating H_2O by F^-.[41] Corresponding data for 1 mM and 100 mM fluoride concentrations can be found in the SI, Figure S9.

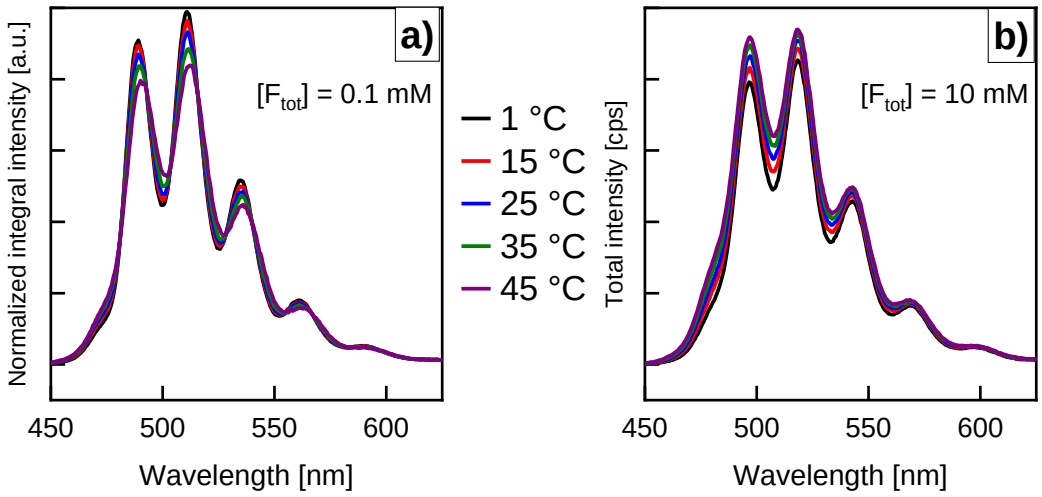

Figure 7: Luminescence spectra of uranyl(VI) ([U] = 0.1 mM) with fluoride at **a)** [F] = 0.1 mM and at **b)** [F] = 10 mM at 1 – 45 °C; I = 1 M; −log[H] = 2.

The apparent increasing fluoride complexation with increasing temperature observed in the present work are in contrast with published results by Kirishima et al. (2004), who indicated that an increasing temperature would decrease U(VI)-fluoride complexation[15]. In a more recent study by Tian et al. (2009), the opposite was observed for all four investigated $UO_2F_n^{2-n}$ complexes, in agreement with the results obtained in the present study.[16] From our results we can conclude that fluoride does not quench the luminescence of uranyl(VI) even at elevated temperatures. The luminescence lifetimes of the uranyl(VI) fluoride complexes are longer than

the uranyl(VI) aquo ion lifetime, which indicate a lack of quenching caused by the fluoride anion.

The situation is very different for chloride. At the same low halide concentration of 10 mM, the U(VI) luminescence signal is reduced by almost 97 % in the presence of chloride in comparison to the aquo ion (Figure S1). Thus, dynamic quench processes play a large role in the quench reaction. In addition, the UO_2Cl^+ is likely to contribute to static quench effects. As dynamic quenching is temperature dependent and the formation of the UO_2Cl^+ complex is endothermically driven[11] and will be favored with increasing temperature, the quench process has been investigated in the 1 – 45 °C temperature range using Stern-Volmer analysis.[28] The Stern-Volmer equation (5) describes the ratio of unquenched luminescence I_0 to quenched luminescence I in relation to the quencher concentration [Q]. Those parameters are connected by the Stern-Volmer constant K_{SV}, which is a measure of the amount of quenching.

$$\frac{I_0}{I} - 1 = K_{SV} \cdot [Q] \tag{5}$$

As already mentioned, two quenching processes can be distinguished: dynamic and static quenching. During dynamic quenching a bimolecular collision between an excited fluorophore and a quenching molecule takes place, which results in an energy loss of the fluorophore without emission of luminescence. Static quenching describes a process, in which a fluorophore forms a complex with the quencher, thereby creating a non-luminescent complex.

To determine which quenching process occurs in solution the chloride concentration is plotted against I_0/I and τ_0/τ, where τ_0 describes the lifetime of the fluorophore without quencher and τ with a quencher present. In the case of purely dynamic quenching I_0/I equals τ_0/τ, whereas in a purely static quenching process τ_0/τ is always one. To investigate the quenching process solutions containing uranyl(VI) ([U] = 0.1 mM) and chloride ([Cl] = 0 – 0.1 M) were prepared at a $-\log[H]$ of 1 with an ionic strength of 0.11 M. To obtain I_0/I and τ_0/τ the static luminescence spectra and the luminescence lifetimes of the uranyl(VI) at varying chloride concentration are required.

From the static luminescence spectra in Figure 8 a) at 1 °C and b) at 45 °C it becomes evident, that the luminescence intensity of the uranyl(VI) decreases with increasing chloride concentration and increasing temperature. Similarly, the luminescence lifetime in Figure 8, measured at c) 1 °C and d) 45 °C, decreases with increasing chloride concentration and increasing temperature. Lifetimes with chloride concentrations greater than 5 mM show a biexponential decay, indicating the presence of two uranyl(VI) species in solution: the

uranyl(VI) aquo ion and the former observed UO_2Cl^+ complex. This observation agrees with our speciation data obtained at –120 °C. The complex shows a luminescence lifetime, which is at 25 °C much shorter (8 ± 3 ns) than the lifetime of its fluoride analogue (41 ± 15 µs).

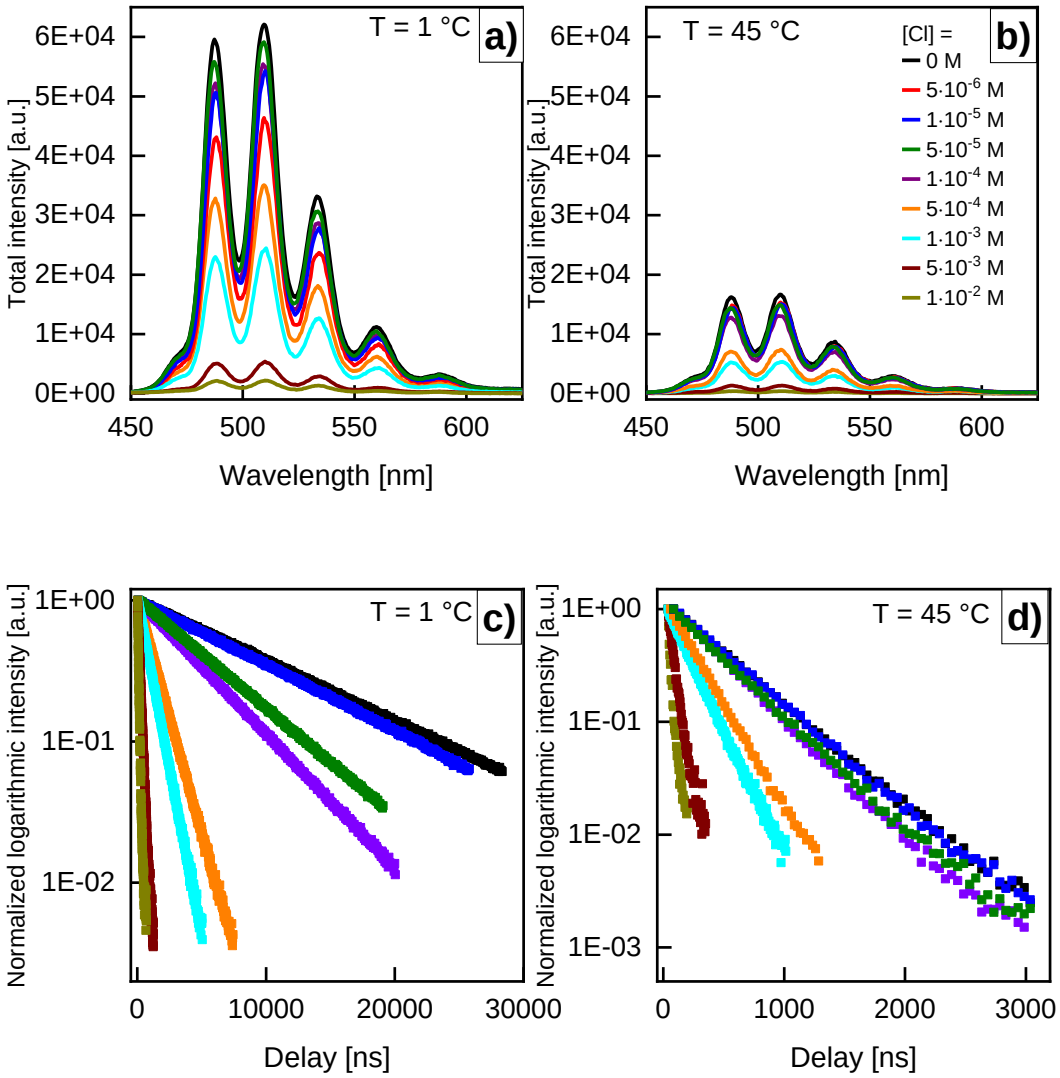

Figure 8: Luminescence spectra of the uranyl(VI) luminescence ([U] = 0.1 mM) with chloride ([Cl] = 0 – 0.01 M) at **a)** 1 °C and **b)** 45 °C. Recorded lifetimes of the uranyl(VI) luminescence intensity of the same samples at **c)** 1 °C and **d)** 45 °C at −log[H] = 1 and I = 0.11 M.

Generally two trends can be observed from plotting I_0/I and τ_0/τ against the chloride concentration at different temperatures: with increasing temperature a less linear behavior for I_0/I against [Cl] is observed in Figure 9 a), indicating the existence of primarily dynamic quenching at lower temperatures and additionally static quenching at elevated temperatures. This is further supported by Figure 9 b), which shows that τ_0/τ against [Cl] is getting smaller with increasing temperature and the linearity decreases, indicating the presence of static quenching besides dynamic quenching at higher temperatures. This is not surprising, since

Awasthi et al. have determined the formation of UO_2Cl^+ to be an endothermic reaction ($\Delta_r H^\circ_m = 8 \pm 2$ kJ mol^{-1}), meaning complex formation is favored at higher temperatures.[11]

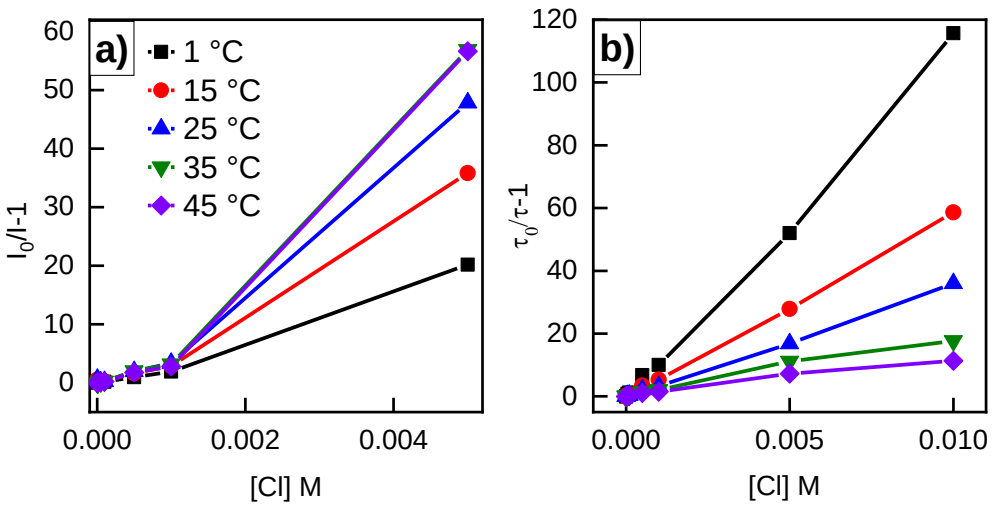

Figure 9: **a)** Ratios of the static luminescence intensity I_0/I and **b)** ratios of the luminescence lifetimes τ_0/τ against the chloride concentration at 1 to 45 °C.

To differentiate between the observed static and dynamic quench processes, K_{SV} is divided into a Stern-Volmer constant for dynamic quenching K_d and static quenching K_s according to equation (S1). By rewriting the equation as presented in equation (S2), a linear regression obtained by plotting the known values for $\left(\frac{I_0}{I} - 1\right) \cdot \frac{1}{[Q]}$ against [Q] will yield K_dK_s as the slope and $K_d + K_s$ as the intercept with the y-axis, from which K_d and K_s can be derived. The results of the linear regression for all investigated temperatures can be found in the SI, Figure S10. The obtained values for the dynamic and static quenching are presented in Table S7. By comparing K_d with K_s it becomes obvious, that dynamic quenching is approximately two to five times higher than static quenching, meaning that dynamic quenching has a bigger impact on the overall quenching process. From the K_d it is possible to determine the bimolecular quenching constant k_q using equation (6), which describes the possibility of collisional quenching in solution to occur.

$$K_d = \tau_0 \cdot k_q \qquad (6)$$

k_q was determined for temperatures from 1 – 45 °C as presented in Table S8, which shows that the event of a collisional quenching increases exponentially with increasing temperature. At 25 °C in 0.11 M $NaClO_4$, $-\log[H] = 1.0$, a k_q value of 1.16×10^9 M^{-1}s^{-1} was found. This value is in very good agreement with published values for the k_q in chloride containing media. Yokoyama et al. (1976) found a k_q value of 1.7×10^9 M^{-1}s^{-1} in 1 M $HClO_4$.[22] A value of

1.8×10^9 $M^{-1}s^{-1}$ was reported in 3 M $NaClO_4$ at pH = 3.4 by Park et al. (1990).[42] As our investigations were conducted at a significantly lower ionic strength (0.11 M), a lower k_q value is expected for the quench process.[43-46] The k_q value obtained in this work is comparable to quench constants found for 10 mM U(VI) solutions in 1 M $HClO_4$ in the presence of metal ions in their reduced oxidation states (e.g. 1.0×10^9 for Fe^{2+}, 4.5×10^9 for Tl^+) and several orders of magnitude larger than corresponding values for metal ions in their oxidized oxidation states (2.2×10^6 for Fe^{3+}, 8.7×10^7 for Tl^{3+}).[47] This implies that the redox-reactions resulting in U(VI) reduction to U(V) and/or U(IV) and subsequent oxidation of Fe or Tl are comparable to the photoinduced "reduction" of U(VI) by the chloride ligand resulting in non-luminescent U(V)-like excited state.

Finally, the temperature dependence of k_q can be used to calculate the activation energy of the quenching process using the logarithm of the Arrhenius equation (S3).[48] Using a linear fit, the activation energy E_a and the pre-exponential factor A can be obtained from the slope and the intercept with the y-axis, respectively. The resulting plot is shown in Figure 10 a and results in E_a = 55.0 ± 12.9 kJ mol^{-1} or 0.592 ± 0.134 eV and A = $(1.47 \pm 0.09)\times10^{19}$ s^{-1} (Table 5). E_a describes the amount of energy that is required to form the transition state, called the collisional complex, between the excited uranyl(VI) and the chloride. The activation energy determined experimentally in this work is of the same order of magnitude as an estimated value of 0.11 eV from Yokoyama et al.[22] It is slightly larger than activation energies reported for UO_2^{2+} in aqueous solution containing various concentrations of $HClO_4$/$NaClO_4$ (see summary in Allsopp et al. (1979)) which range from 23.9 to 51.9 kJ mol^{-1}.[49] However, the pre-exponential factor is almost 6 to 8 magnitudes larger in chloride solution in comparison to other common media containing e.g. fluoride or perchlorate, which explains the much higher influence of chloride on the quenching of uranium(VI) luminescence in comparison to aqueous solutions containing non-quenching ligands such as perchlorate. Further information of the quench process can be obtained by applying the Eyring equation (S4).[50] Using equation (S4) as a linear fit, the activation enthalpy $\Delta H^{\ddagger}$ can be obtained by the slope and the activation entropy $\Delta S^{\ddagger}$ by the intercept with the y-axis (see Figure 10 b). $\Delta H^{\ddagger}$ was calculated to be 52.5 ± 13.0 kJ mol^{-1} or 0.567 ± 0.135 eV, while $\Delta S^{\ddagger}$ is 103.9 ± 42.8 J mol^{-1} K^{-1} or $1.1\cdot10^{-3} \pm 0.4\cdot10^{-3}$ eV K^{-1}. Because the enthalpy and entropy terms are both positive, the energy barrier between the reactants and the transition state is lowered with increasing temperature. Since the transitions state formation is favored, this directly increases the dynamic quenching of the uranyl(VI) luminescence through chloride in the system. In two different studies Marcantonatos and Deschaux reported activation enthalpy and entropy values for the quenching process of uranyl(VI) with Ag^+ and

Tl^+.[46, 51] The activation enthalpy $\Delta H^{\ddagger}(Ag^+)$ was decreasing with increasing ionic strength (I = 0.019 – 0.1 M) from 36.9 to 36.5 kJ mol^{-1}, while the activation entropy $\Delta S^{\ddagger}(Ag^+)$ increased from 2.3 to 4.6 J mol^{-1} K^{-1}. For Tl^+ at I = 0.034 M an activation enthalpy of 13.89 kJ mol^{-1} and entropy of 23.4 J mol^{-1} K^{-1} was determined. The resulting k_q for both metals were in the same order of magnitude as the value obtained for chloride in this work being $k_q(Ag^+$; I = 0.019 – 0.1 M) = (1.96 – 2.51)×10^9 and $k_q(Tl^+) = 1.6\times10^9$. This shows that while the energy barrier $\Delta H^{\ddagger}$ for the quenching process with Ag^+ and Tl^+ might be lower, the entropic term $\Delta S^{\ddagger}$ in systems with chloride is much larger, therefore resulting in similar k_q values.

Table 5: Determined thermodynamic parameters by applying Arrhenius and Eyring equations.

Arrhenius equation	**Pre-exponential factor A [s^{-1}]**	**Activation energy E_a [kJ mol^{-1} | eV]**
	(1.47 ± 0.09)×10^{19}	55.0 ± 12.9 | 0.592 ± 0.134
Eyring equation	**Activation enthalpy $\Delta H^{\ddagger}$ [kJ mol^{-1} | eV]**	**Activation entropy $\Delta S^{\ddagger}$ [J mol^{-1} K^{-1} | eV K^{-1}]**
	52.5 ± 13.0 | 0.567 ± 0.135	103.9 ± 42.8 | 1.1·10^{-3} ± 0.4·10^{-3}

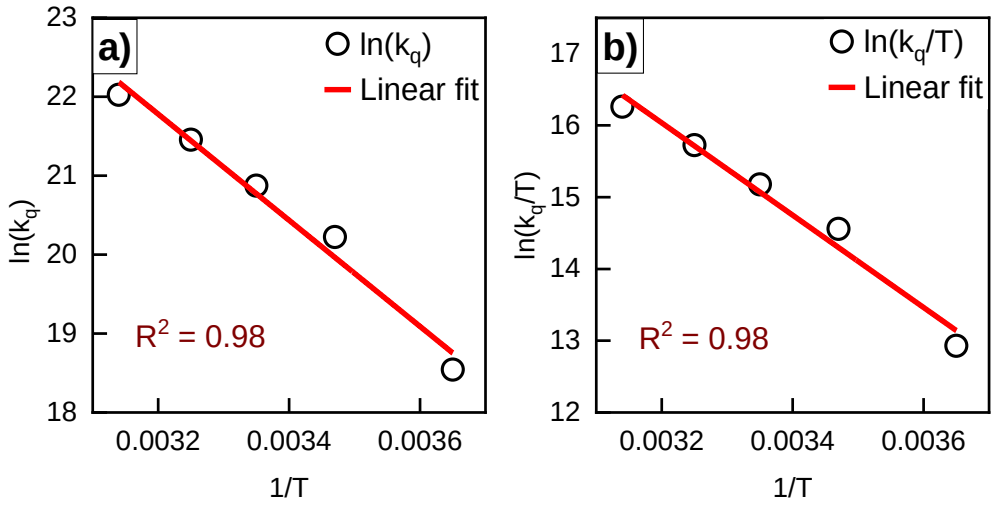

Figure 10: Linear fits of the **a)** logarithmic Arrhenius equation (S3) and **b)** logarithmic Eyring (S4).

4 Conclusions

Using TRLFS we were able to present pure component luminescence spectra for the UO_2F^+, UO_2F_2, $UO_2F_3^-$ and $UO_2F_4^{2-}$ complexes at 25 °C in the aqueous uranyl(VI) fluoride system. From the pure component spectra it was possible to obtain the species distribution, from which we determined the log$K$* values at 25 °C and I = 1 M for the above mentioned complexes for the first time using TRLFS as an analytical method and performed an extrapolation to obtain the logK^0 values at infinite dilution. The obtained results were comparable to the latest existing literature values determined by other analytical methods, which investigated the same uranyl(VI) fluoride ($UO_2F_n^{2-n}$; n = 4) complexes. A spectrum of a uranyl(VI) complex with five coordinating fluoride has yet to be obtained using TRLFS and is of interest for future investigations. In the uranyl(VI) chloride system spectral deconvolution of luminescence spectra yielded the very first pure component luminescence spectra of UO_2Cl^+ at −120 °C and at 1 °C. The uranyl(VI) chloride complex shows luminescence bands in the same region as the UO_2F^+ complex, indicating a similar complex structure between uranyl(VI) and the two halides, although the log$K$ values show that UO_2F^+ is more stable than the UO_2Cl^+ complex. Knowledge of the pure component spectrum of UO_2Cl^+ will provide valuable information for future investigations of the uranyl(VI) luminescence in chloride bearing systems. The slope analysis of the uncorrected U(VI)-chloride species distribution showed that the stoichiometry of the formed complex corresponds to the UO_2Cl^+ complex. This is the first time information of a complex stoichiometry has been derived at liquid nitrogen temperatures. This shows that the challenge of chloride quenching of uranyl(VI) can be overcome by freezing the sample, allowing investigations of uranyl(VI) luminescence in (natural) media containing chloride. More work, however, is required to be able to obtain reliable relative luminescence quantum yields (LI factors) of frozen samples to be used in the correction of the species distribution and the subsequent calculation of the complexation constant using slope analysis.

Temperature dependent studies in the uranyl(VI) fluoride system showed, that at higher temperatures uranyl(VI) fluoride complex formation is favored. This generally leads to an increase in luminescence intensity due to replacement of quenching water molecules with fluoride. Hence, no indications for temperature-dependent quenching for uranyl-fluoride complexes could be established. Further, the uranyl(VI) chloride system was investigated at different temperatures using Stern-Volmer analysis. The chloride induces an overall strong quenching of the uranyl(VI) luminescence, caused by static and dynamic quenching effects. Static quenching increases at higher temperatures due to enhanced complexation taking place in solution. The contribution of the dynamic quenching to the overall quenching effect is two

to five times larger than the contribution of the static quenching. From the K_d values we calculated the bimolecular quenching constants k_q at 1 to 45 °C, which show an exponential increase with increasing temperature. Applying the Arrhenius and the Eyring equations we obtained the activation energy, activation entropy, and activation enthalpy of the dynamic quench process. The results show that with increasing temperature the energetic barrier between the transition state of the excited uranyl(VI) and chloride is lowered, therefore increasing the quenching effect.

Acknowledgements

The authors would like to thank the German Federal Ministry of Education and Research (BMBF) for funding the ThermAc (02NUK039B) project. The authors kindly acknowledge funding by the German Ministry of Economic Affairs and Energy under the grants 02E11334B within the EDUKEM project: Development and application of experimental techniques to improve modelling of saline uranium containing solutions. We want to thank Stephan Weiss and Dr. Björn Drobot for their help in this study.

5 References

1. Y. K. Kharaka, A. S. Maest, W. W. Carothers, L. M. Law, P. J. Lamothe and T. L. Fries, *Applied Geochemistry*, 1987, **2**, 543-561.
2. K. Bucher, Y. Zhu and I. Stober, *International Journal of Earth Sciences*, 2009, **98**, 1727-1739.
3. F. Pearson, D. Arcos, A. Bath, J. Boisson, A. M. Fernández, H. Gäbler, E. Gaucher, A. Gautschi, L. Griffault and P. Hernán, *Report of the Swiss Federal Office for Water and Geology, Geology Series*, 2003, **5**, 319.
4. D. E. Harlov, V. Procházka, H.-J. Förster and D. Matějka, *Mineralogy and Petrology*, 2008, **94**, 9-26.
5. J. E. Gagnon, I. M. Samson, B. J. Fryer and A. E. Williams-Jones, *The Canadian Mineralogist*, 2003, **41**, 365-382.
6. G. Y. Grigor'ev, S. S. Nabiev, S. L. Malyugin, M. A. Sukhanova, A. I. Nadezhdinskii and Y. Y. Ponurovskii, *Atomic Energy*, 2009, **105**, 280.
7. K. Elam, *ORNL/TM-2003/239, UT-Battelle, LLC, Oak Ridge National Laboratory, Oak Ridge, TN*, 2003.
8. S. Ahrland, *Acta Chemica Scandinavica*, 1951, **5**, 1271-1282.
9. S. Ahrland, *Acta Chemica Scandinavica*, 1956, **10**, 705-718.
10. V. N. Krylov, E. V. Komarov and M. F. Pushlenkov, *Sov. Radiochem.*, 1968, **10**, 708-710.
11. S. P. Awasthi and M. Sundaresan, *Indian Journal of Chemistry Section a-Inorganic Bio-Inorganic Physical Theoretical & Analytical Chemistry*, 1981, **20**, 378-381.
12. F. Nelson and K. A. Kraus, *Journal of the American Chemical Society*, 1951, **73**, 2157-2161.
13. W. D. Bale, E. W. Davies, D. B. Morgans and C. B. Monk, *Discussions of the Faraday Society*, 1957, 94-102.
14. H. Ohashi and T. Morozumi, *Nippon Genshiryoku Gakkaishi*, 1967, **9**, 65-71.
15. A. Kirishima, T. Kimura, O. Tochiyama and Z. Yoshida, *Radiochim. Acta*, 2004, **92**, 889-896.
16. G. Tian and L. Rao, *Inorg. Chem.*, 2009, **48**, 6748-6754.
17. S. Bauer, C. Beyer, F. Dethlefsen, P. Dietrich, R. Duttmann, M. Ebert, V. Feeser, U. Görke, R. Köber, O. Kolditz, W. Rabbel, T. Schanz, D. Schäfer, H. Würdemann and A. Dahmke, *Environmental Earth Sciences*, 2013, **70**, 3935-3943.
18. A. Skerencak, P. J. Panak, V. Neck, M. Trumm, B. Schimmelpfennig, P. Lindqvist-Reis, R. Klenze and T. Fanghanel, *Journal of Physical Chemistry B*, 2010, **114**, 15626-15634.
19. S.-i. Ishiguro, C.-F. Kao and H. Kakihana, *Denki Kagaku*, 1977, **45**, 651-653.
20. R. M. Sawant, N. K. Chaudhuri, G. H. Rizvi and S. K. Patil, *Journal of Radioanalytical and Nuclear Chemistry*, 1985, **91**, 41-58.
21. V. M. Vdovenko and O. B. Stebunov, *Sov. Radiochem.*, 1969, **11**, 630-632.
22. Y. Yokoyama, M. Moriyasu and S. Ikeda, *Journal of Inorganic & Nuclear Chemistry*, 1976, **38**, 1329-1333.
23. H. D. Burrows, *Inorg. Chem.*, 1990, **29**, 1549-1554.
24. S. Tsushima, C. Gotz and K. Fahmy, *Chemistry-a European Journal*, 2010, **16**, 8029-8033.
25. T. Haubitz, S. Tsushima, R. Steudtner, B. Drobot, G. Geipel, T. Stumpf and M. U. Kumke, *The Journal of Physical Chemistry A*, 2018, **122**, 6970-6977.
26. R. Steudtner, S. Sachs, K. Schmeide, V. Brendler and G. Bernhard, *Radiochimica Acta International journal for chemical aspects of nuclear science and technology*, 2011, **99**, 687-692.

27. R. Steudtner, T. Arnold, G. Geipel and G. Bernhard, *Journal of radioanalytical and nuclear chemistry*, 2010, **284**, 421-429.
28. J. R. Lakowicz, *Principles of fluorescence spectroscopy*, Second edition. New York : Kluwer Academic/Plenum, [1999] ©1999, 1999.
29. N. Jordan, M. Demnitz, H. Lösch, S. Starke, V. Brendler and N. Huittinen, *Inorg. Chem.*, 2018, **57**, 7015-7024.
30. D. L. Parkhurst and C. A. J. Appelo, *Description of input and examples for PHREEQC version 3: a computer program for speciation, batch-reaction, one-dimensional transport, and inverse geochemical calculations*, Report 6-A43, Reston, VA, 2013.
31. E. Giffaut, M. Grivé, P. Blanc, P. Vieillard, E. Colàs, H. Gailhanou, S. Gaboreau, N. Marty, B. Madé and L. Duro, *Applied Geochemistry*, 2014, **49**, 225-236.
32. M. Grivé, L. Duro, E. Colàs and E. Giffaut, *Applied Geochemistry*, 2015, **55**, 85-94.
33. I. Grenthe, H. Wanner, I. Forest and O. N. E. Agency, *Chemical thermodynamics of uranium*, North-Holland, 1992.
34. D. Palmer, R. Guillaumont, T. Fanghaenel, V. Neck, J. Fuger, I. Grenthe and M. H. Rand, *Chemical Thermodynamics Vol. 5: Update on the Chemical Thermodynamics of Uranium, Neptunium, Plutonium, Americium, and Technetium*, 2003.
35. N. Huittinen, T. Rabung, A. Schnurr, M. Hakanen, J. Lehto and H. Geckeis, *Geochimica et Cosmochimica Acta*, 2012, **99**, 100-109.
36. S. Ahrland and L. Kullberg, *Acta Chem. Scand.*, 1971, **25**, 3457-3470.
37. C. Nguyen-Trung, D. A. Palmer, G. M. Begun, C. Peiffert and R. E. Mesmer, *Journal of Solution Chemistry*, 2000, **29**, 101-129.
38. C. Götz, G. Geipel and G. Bernhard, *Journal of Radioanalytical and Nuclear Chemistry*, 2011, **287**, 961-969.
39. R. Billing, G. V. Zakharova, L. S. Atabekyan and H. Hennig, *Journal of Photochemistry and Photobiology A: Chemistry*, 1991, **59**, 163-174.
40. R. Nagaishi, T. Kimura, J. Inagawa and Y. Kato, *Journal of Alloys and Compounds*, 1998, **271-273**, 794-798.
41. S. Ahrland and L. Kullberg, *Acta Chemica Scandinavica*, 1971, **25**, 3471-3483.
42. Y. Y. Park, Y. Sakai, R. Abe, T. Ishii, M. Harada, T. Kojima and H. Tomiyasu, *Journal of the Chemical Society-Faraday Transactions*, 1990, **86**, 55-60.
43. N. Miyoshi, M. Ueda, K. Fuke, Y. Tanimoto, M. Itoh and G. Tomita, *Zeitschrift für Naturforschung B*, 1982, **37**, 649-652.
44. M. A. Rubio, D. O. Mártire, S. E. Braslavsky and E. A. Lissi, *Journal of Photochemistry and Photobiology A: Chemistry*, 1992, **66**, 153-157.
45. H. D. Burrows, S. J. Formosinho, M. D. G. Miguel and F. P. Coelho, *Journal of the Chemical Society, Faraday Transactions 1: Physical Chemistry in Condensed Phases*, 1976, **72**, 163-171.
46. M. Marcantonatos and M. Deschaux, *Chemical Physics Letters*, 1980, **76**, 359-365.
47. M. Moriyasu, Y. Yokoyama and S. Ikeda, *Journal of Inorganic and Nuclear Chemistry*, 1977, **39**, 2205-2209.
48. S. Arrhenius, *Zeitschrift für physikalische Chemie*, 1889, **4**, 226-248.
49. S. R. Allsopp, A. Cox, T. J. Kemp, W. J. Reed, V. Carassiti and O. Traverso, *Journal of the Chemical Society, Faraday Transactions 1: Physical Chemistry in Condensed Phases*, 1979, **75**, 342-352.
50. H. Eyring, *The Journal of Chemical Physics*, 1935, **3**, 107-115.
51. M. Deschaux and M. Marcantonatos, *Journal of Inorganic and Nuclear Chemistry*, 1981, **43**, 2915-2917.